Solar Energy Materials and Solar Cells 178 (2018) 46–51

Contents lists available at ScienceDirect

Solar Energy Materials and Solar Cells

journal homepage: www.elsevier.com/locate/solmat

Imaging, microscopic analysis, and modeling of a CdTe module degraded by heat and light

Steve Johnston[a,*], David Albin[a], Peter Hacke[a], Steven P. Harvey[a], Helio Moutinho[a], Chun-Sheng Jiang[a], Chuanxiao Xiao[a], Anuja Parikh[b], Marco Nardone[b], Mowafak Al-Jassim[a], Wyatt K. Metzger[a]

[a] *National Renewable Energy Laboratory, Golden, CO 80401, USA*
[b] *Bowling Green State University, Bowling Green, OH, USA*

ARTICLE INFO

Keywords:
Accelerated aging
Cadmium telluride
Imaging, microscopy
Modeling
Photoluminescence

ABSTRACT

Photoluminescence (PL), electroluminescence (EL), and dark lock-in thermography are collected during stressing of a CdTe module under one-Sun light at an elevated temperature of 100 °C. The PL imaging system is simple and economical. The PL images show differing degrees of degradation across the module and are less sensitive to effects of shunting and resistance that appear on the EL images. Regions of varying degradation are chosen based on avoiding pre-existing shunt defects. These regions are evaluated using time-of-flight secondary ion-mass spectrometry and Kelvin probe force microscopy. Reduced PL intensity correlates to increased Cu concentration at the front interface. Numerical modeling and measurements agree that the increased Cu concentration at the junction also correlates to a reduced space charge region.

1. Introduction

Imaging techniques such as electroluminescence (EL) [1] and photoluminescence (PL) [2,3] are used for their quick acquisition and ability to spatially resolve quality, performance, and defects in photovoltaic cells and modules. For PL and EL imaging, intensity is proportional to radiative recombination of excess carriers. When doping is assumed to be constant, PL and EL imaging can show spatial variation of parameters that affect carrier recombination and are proportional to cell parameters, such as open-circuit voltage. Relatively dark areas suggest that performance is decreased due to carrier recombination through impurities, defect states, or shunts. When excess carriers are uniformly generated by optical excitation, PL imaging is less dependent on series resistance. EL imaging relies on electrical carrier injection, so images can be affected by defects for carrier recombination and high resistance or shunts that prevent uniform carrier injection throughout the cell.

When imaging lower bandgap materials such as Si and $CuIn_xGa_{1-x}Se_2$, Si-based cameras detect luminescence at the edge of their sensitivity range, but provide very reasonable results for less cost than InGaAs-based cameras. For PL imaging, the light source is ideally monochromatic, such as 808-nm laser diodes, or light-emitting diodes for less-demanding applications like well-passivated materials or high-quality cells. For larger bandgap materials such as CdTe, the PL emission occurs in a more sensitive region of Si-based cameras, which gives a stronger signal for the less expensive camera types. However, the shorter wavelength laser sources needed for excitation can significantly increase the cost of a PL imaging tool.

We have constructed an economical PL imaging system using a green 532-nm laser diode with a raster of the laser beam for large area samples. Here, we couple this work with EL, dark lock-in thermography (DLIT), time-of-flight secondary ion mass spectrometry (TOF-SIMS), and Kelvin probe force microscopy (KPFM) on ~ 1.5 eV, high-bandgap CdTe modules stressed under light and heat. We are able to detect non-uniform degradation in CdTe mini-modules correlated with Cu concentration at the front interface. 2D numerical modeling of performance degradation and copper diffusion is employed to provide a mechanistic analysis of the data.

2. Imaging

The PL imaging system uses a 532-nm laser diode from Laserglow Technologies, and the laser beam is swept in a raster pattern using a pair of scanning galvanometer mirrors from Thor Labs. In one direction, the beam is quickly scanned back and forth (~ 300 Hz) to form a line, and this laser line is slowly swept in the orthogonal direction (~ 0.1 Hz)

---

[*] Corresponding author.
E-mail address: steve.johnston@nrel.gov (S. Johnston).

https://doi.org/10.1016/j.solmat.2017.12.021
Received 28 September 2017; Received in revised form 22 November 2017; Accepted 17 December 2017

over an area larger than the sample (~ 20 × 20 cm mini-module studied here). The intensity is adjusted by varying the duty cycle when using a pulse width modulation at a frequency of 10 kHz. The typical laser power during a PL measurement is roughly 0.5–1 mW for a beam spot size of ~ 1 mm diameter. This is equivalent to approximately 100 mW/cm^2. A Princeton Instruments PIXIS 1024BR charge-coupled device (CCD) camera is used for collecting PL and EL images, although the enhanced near-infrared efficiency is not needed for the CdTe luminescence wavelength range. This Si camera collects the PL image with a long exposure time (~ 1–2 min) that is a multiple of the 10-second period of the laser raster time. A stack of three RG715 Schott glass filters is mounted to the camera lens to block scattered laser light and allow the CdTe PL to be transmitted. The cells of the mini-module are several millimeters in width. EL images are collected by driving forward-bias current, which is about 1/3 of J_{SC} (short-circuit current), through the module. DLIT images are collected with a Cedip Silver 660 M (FLIR SC5600-M) InSb camera having lock-in data acquisition. The forward-bias current, also approximately 1/3 of J_{SC}, is pulsed at a frequency of 0.1 Hz, which allows for a better thermal signal through the mini-module's 3-mm-thick glass.

A CdTe mini-module for testing and characterization was obtained through an industrial source and had not undergone any stress prior to our tests. It is produced using a commercial process that is scalable to production quantities. It has a standard polycrystalline film stack, and after fabrication, it has more Cu near the back surface. The CdTe module is initially characterized by imaging before stresses are applied. Fig. 1(a)–(c) show PL, EL, and DLIT images for the initial state of the module. The PL image of Fig. 1(a) shows that the module is mostly uniform with only a few spatially-localized defects or anomalies. The EL image, Fig. 1(b), shows that the upper three-quarters of the module are slightly darker. This is most likely due to the shunting defects seen in the DLIT image (Fig. 1(c)) indicating a large number of shunting defects that are also mostly present in the central/upper half of the module. Elevated temperatures are represented by higher intensity signals, shown here by orange and yellow colors. Blue colors represent the lowest temperatures, and red shades are in-between temperatures. Because the EL is collected with only ~ 1/3 of the J_{SC} current expected at 1 sun, the shunts within each cell can reduce the EL emission by dropping the voltage across that cell. The currents applied during the imaging were intentionally kept low to reduce the risk of generating new defects or accelerating defect degradation during the study.

The module was stressed by subjecting it to one-Sun light exposure at an elevated temperature of 100 °C. A hotplate only slightly larger than the module was used for heating. Consequently, the edges of the module were approximately 15% cooler relative to the center which was maintained at 100 °C. Dark and light current-voltage curves were measured periodically. The module parameters from the measurements are shown in Fig. 2. The open-circuit voltage, V_{OC}, consistently drops over the time of stressing. The fill factor and efficiency initially show slight improvement before later decreasing. The short-circuit current, J_{SC}, remains fairly constant throughout the stress time.

The module was also periodically imaged during the stressing time. EL images began to show more contrast, with the upper-right two-thirds of the cell appearing dark, after just 5 h of stress. The PL images began to show a darker region in the center, likely due to the non-uniform heating during stress, after about 60 h of stress. The final images after 400 h of stress are shown in Fig. 1(d)–(f). The EL image, Fig. 1(e), again shows more contrast with dark regions due to both shunting in the upper half and degradation in the center region that also appears dark in the PL image, Fig. 1(d). The DLIT image, Fig. 1(f), shows that the shunts have become more pronounced during stress. Based on the images, regions of least, middle, and most degradation are chosen where shunting and initial defects are not apparent in the DLIT image. These areas are represented by green, orange, and red circles, where the

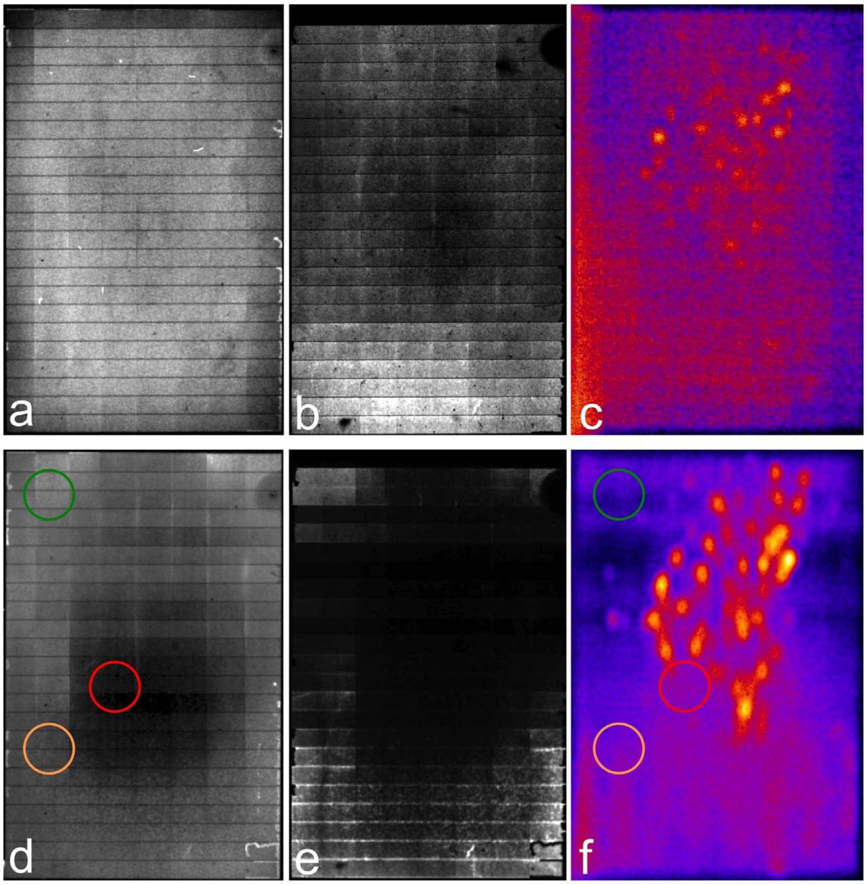

Fig. 1. Pre-stress images of the CdTe module show (a) PL, (b) EL, and (c) forward-bias DLIT. Post-stress images of the CdTe module show (d) PL, (e) EL, and (f) DLIT. Circles (green for least degraded and red for most degraded) mark regions of interest away from shunts, where PL imaging shows various degrees of degradation. (For interpretation of the references to color in this figure legend, the reader is referred to the web version of this article.)